1 **Title:**
2 Binding during sequence learning does not alter cortical representations of individual actions
3
4 **Authors:**
5 Patrick Beukema[1,2], Jörn Diedrichsen[3] and Timothy Verstynen[4,2]
6 [1]Center for Neuroscience, University of Pittsburgh, Pittsburgh, Pennsylvania, 15260
7 [2]Center for the Neural Basis of Cognition, University of Pittsburgh & Carnegie Mellon
8 University, Pittsburgh, Pennsylvania, 15213
9 [3]Brain and Mind Institute, Departments of Statistics & Computer Science, University of Western
10 Ontario
11 [4]Department of Psychology, Carnegie Mellon University, Pittsburgh, Pennsylvania, 15213
12
13
14 **Corresponding author:**
15 Timothy Verstynen
16 Department of Psychology
17 Carnegie Mellon University
18 Pittsburgh, Pennsylvania, 15213
19 email: timothyv@andrew.cmu.edu
20
21 Pages: 30
22 Figures: 5
23 Tables: 3
24
25 Number of words
26 Abstract: 148
27 Introduction: 718
28 Discussion: 694
29
30 **Conflict of interest:** None
31

ABSTRACT

As a movement sequence is learned, serially ordered actions get bound together into sets in order to reduce computational complexity during planning and execution. Here we examined how the binding of serial actions alters the cortical representations of individual movements. Across five weeks of practice, healthy human subjects learned either a complex 32-item sequence of finger movements (Trained group, N=9) or randomly ordered actions (Control group, N=9). After five weeks of training, responses during sequence production in the Trained group were correlated, consistent with being bound together under a common command. These behavioral changes, however, did not coincide with plasticity in the multivariate representations of individual finger movements, assessed using fMRI, at any level of the cortical motor hierarchy. This suggests that the representations of individual actions remain stable, even as the execution of those same actions become bound together in the context of producing a well learned sequence.

49 **INTRODUCTION**

50   Being able to combine simple movements into coordinated sets of actions is critical to

51   many everyday skills, such as typing on the computer or driving a manual transmission car

52   (Lashley, 1951). Over the course of evolution the brain has solved this sequencing problem

53   multiple times, resulting in many interacting algorithms that facilitate the consolidation of

54   complex skills (for review see Beukema and Verstynen 2018). One of these algorithms is the

55   process of set building, also known as chunking or binding (Verwey 1996). Binding serial

56   actions into sets improves computational efficiency during the production of complex actions by

57   representing multiple movements under a single selection command (Ramkumar et. al, 2016). To

58   illustrate this process consider the graphical model presented in Figure 1A-B. On each trial, the

59   manual response to a visual cue occurs through a hierarchical system of perception, selection

60   (e.g., key), and motor planning (e.g., finger movement), that are all represented as latent states

61   with their own independent sources of noise. In this example, the serial order of cues across trials

62   follows a deterministic sequential order. Prior to training, each response is planned

63   independently of the preceding trial. Once the order of cues is learned, the brain can consolidate

64   the selection process so that a set of motor plans is represented under a single selection state.

65   This selection state is triggered by the presentation of the first stimulus in the series, after which

66   subsequent motor commands are cued by the internal state, rather than by the visual cues. This

67   results in faster production of responses to items within a set, as well as a correlation in

68   responses within bound sets due to their shared upstream command (Figure 1C; Verstynen et al.,

69   2012; Acuna et al., 2014; Lynch et al., 2017).

70
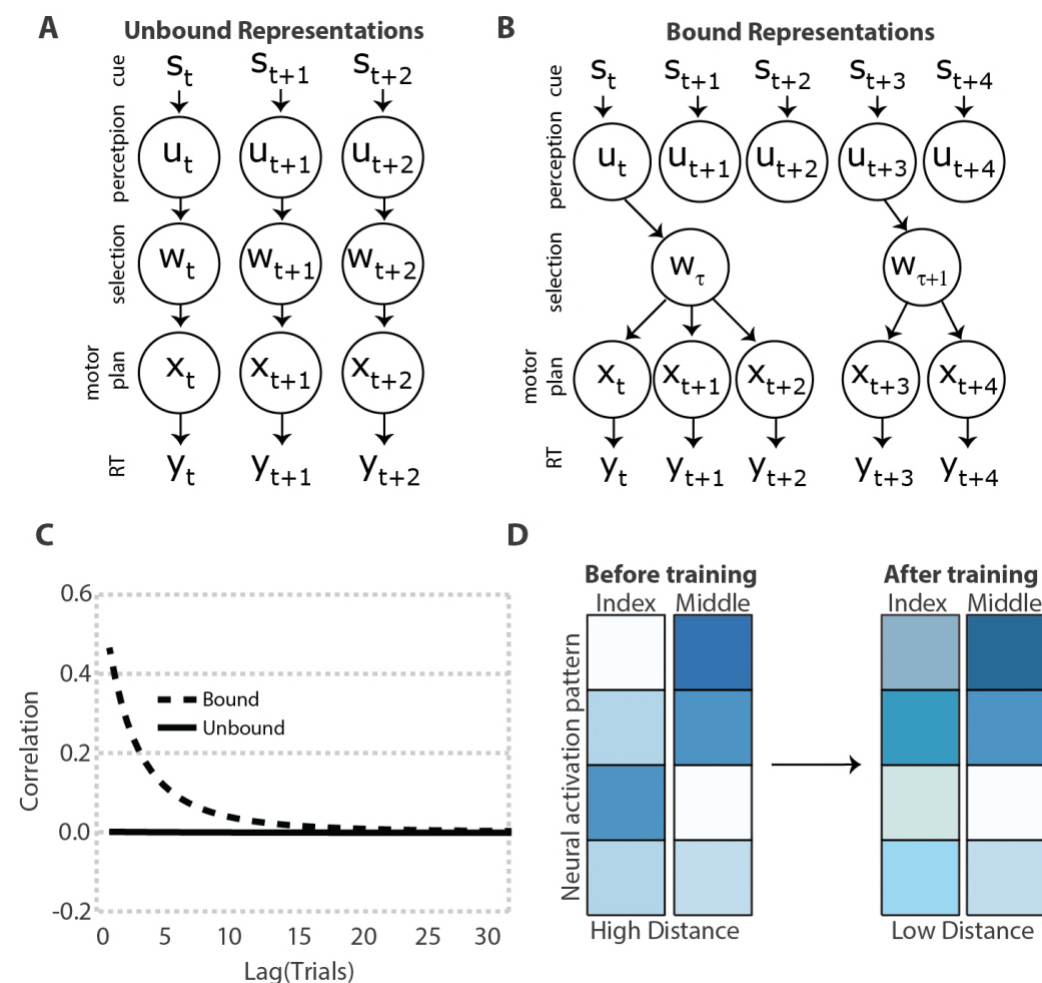
Figure 1: The process of response binding **A**. One each trial, (t), a visual stimulus (s) triggers an appropriate finger response (y), in this case reflecting a response time (RT). In the case of unbound actions, the visual perception (u), selection (w), and motor planning (x) processes are all represented as latent states that operate independently across trials. **B**. With training, the intermediary process of selection binds multiple motor plans together as a set. Each set of actions, τ, is triggered by the visual stimulus of the first item in the set. Subsequent actions are then internally triggered, rather than relying on external visual cues. This example shows two bound sets, a three item set followed by a two item set. **C**. The autocorrelation function of response times for bound actions (cyan) should exhibit a significant correlation across trials, while unbound actions (black) should not exhibit a temporal autocorrelation. **D**. A schematic of four hypothetical voxels in cortical sensory motor networks during the execution of either the index or middling finger, with darker colors reflecting stronger movement-evoked responses. Before training, each finger representation is associated with a unique neural activation pattern. After training, the representations of bound finger movements share more activation and the neural activation patterns are more similar.

86

87   Many forms of non-sequential motor learning rely on the reorganization of movement

88   representations in motor networks (Nudo et. al. 1996). Therefore, it is possible that action

89   binding during sequence learning also alters internal motor representations of individual

90   movements; however, this effect has been largely unexplored. Recent advances in

91   representational analysis now allow precise quantification of the relationship between the

92   cortical activity patterns for single finger movements using fMRI (Diedrichsen and Kriegeskorte,

93   2017). Using this approach, previous work has shown that the structure of individual fingers in

94   primary motor cortex is organized in a way that is consistent with their co-articulation during

95   natural hand movements (Ejaz et. al., 2015). Furthermore, artificial manipulations of pairwise

96   finger correlations, by physically yoking two fingers together, alters the distance between finger

97   representations in primary somatosensory cortex (Kolasinski et. al. 2016). This suggests that

98   elementary sensorimotor representations may be plastic and subject to changes over time and

99   that multivariate pattern analyses on fMRI data are sensitive enough to detect these changes.

100   If individual actions are bound under a common motor command, then the internal

101   representations of those actions, at some level of the motor hierarchy, should change over time in

102   these areas that binding occurs. The naïve version of this model is that if two movements are

103   executed repeatedly in a close temporal sequence, then the activation of one finger movement

104   may already pre-activate the following movement. In the extreme, this model makes the

105   prediction that two fingers that are regularly paired together in everyday actions will become

106   enslaved together over time, thereby reducing behavioral flexibility (Lashley, 1951). It is

107   therefore more likely that the process of binding alters the representation of contextually cued

108   actions in upstream regions linked to more abstract response selection (Diedrichsen and

109   Kornysheva, 2015), such as the dorsal premotor cortex (PMd) or motor regions along the

110   intraparietal sulcus. Wherever this binding process happens, the multivariate activity pattern for

111   the two bound movements should become more similar in that region (Figure 1D).

112   Here we tested the plasticity of individual action representations using a combination of

113   behavioral analysis and event-related fMRI. Binding was measured behaviorally by looking at

114   the degree of correlation between successive behavioral responses after training on a unimanual

115   32-item sequence. We also measured the population-level representations of visually-cued single

116   finger movements in the cortex both before and after five weeks of training on the complex

117   sequence. The simple plasticity hypothesis states that binding of serial actions after consolidation

118   of a motor sequence should make the neural representations for those actions more similar,

119   thereby decreasing the representational distance between them.

120

121   **RESULTS**

122   *Learning-related changes in behavior*

123   Participants executed sequences in a serial reaction time task (Nissen and Bullemer, 1987) on a

124   laptop keyboard, in which each finger press was cued by a unique fractal image (Figure 2A).

125   Subjects learned the mapping of cue to finger press prior to the first day of training. After a key

126   press, the response time, measured as the elapsed time between cue onset and key press, was

127   recorded and the next cue was presented following a 250 ms interval. Each day, participants

128   were tested on trial blocks of random sequences (blocks 1,2,6) or trial blocks composed of a

129   specific 32-element sequence (blocks 3,4,5,7). An additional control group received the same

130   amount of training as the trained group – but here all blocks consisted of random sequences.

131   To assess how training impacted performance, we compared the evolution of response

132   times and accuracy across days for the Trained and Control groups. Figure 2B illustrates all trial-

133   wise responses during a single day for a subject in the Trained group. While responses during

134   random trial blocks (black dots) remained relatively constant, the response times during

135   sequence trial blocks (green dots) get steadily faster with training. The last two trial blocks were

136   used to probe learning across time. On average both the Control (dashed line, Figure 2C) and

137   Trained subjects (dashed line, Figure 2D) exhibited a general improvement in response speeds

138   during the final random trial block (block 6). This general across-session speeding of responses

139   during a trial block with random sequences likely reflects the improved learning of the cue-

140   response mapping across days. During the final sequence block (block 7), however, sequence-

141   specific responses in the Trained group also decreased rapidly across training days. Repeated

142   measures ANOVA indicated a significant block x time effect: $F_{(368,23)} = 15.366$, $p = 7.93$ x 10^{-41},

143   with average response times dropping just below 200ms at the end of training (solid line,

144   Figure 2D). As expected, this effect was not observed in the Control group, $F_{(368,23)} = 0.77$, $p =$

145   0.76, where the final trial block did not contain an embedded sequence (solid line, Figure 2C). In

146   order to capture sequence-specific changes in response speed, we normalized the mean response

147   time for the final trial block (sequence in Trained group, random in Control group) by the mean

148   and variance of response times during trial block 6 (random in both groups; see Methods). This

149   analysis depicts a steady improvement in sequence specific response times across the 5 weeks for

150   the Trained group, with sequence block responses approximately 4 standard deviations faster

151   than the random trial blocks at the end of training (Figure 2E). Repeated measures ANOVA

152   indicated a significant group by time effect, $F_{(368,23)} = 12.79$, $p = 1.67$ x 10^{-34}. Unlike response

153   speed, average accuracy during the final trial block gradually rose at a steady rate for both

154   groups, saturating at around 90% for the Trained group and 85% for the Control group, with no

155   significant between group differences $F_{(368,23)} = 0.36$, $p = 0.99$.

7
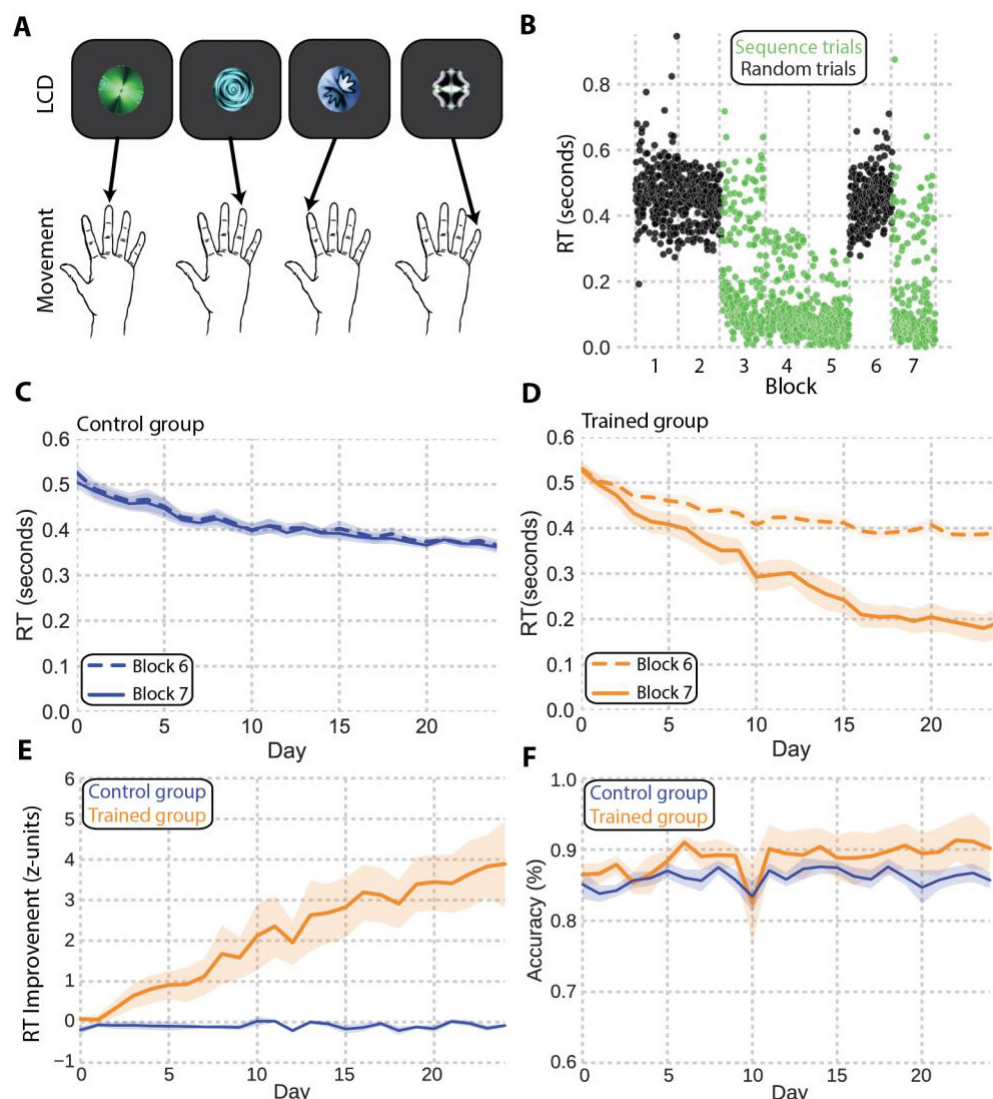
Figure 2: *Task design and behavioral performance.* **A.** *Participants practiced a serial reaction time task in which each finger movement was prompted by a unique cue.* **B.** *Representative reaction time plot from Day 12. Each dot represents the response time on one trial.* **C.** *Reaction times for the Control group for random trials on blocks 6 and 7.* **D.** *Reaction times for the Trained group for the random trials (block 6) and sequence trials (block 7).* **E.** *Mean z-scored reaction times as a function of day for the Control group (blue) and Trained group (peach).* **F.** *Mean accuracy (correct trials/total trials) in the final trial block, as a function of day, for the Control group (blue) and Trained (peach) group. Shaded regions in panels C-F show standard error.*

There are several ways that responses could get faster during the sequence blocks (see

Beukema and Verstynen, 2018). The binding hypothesis (Figure 1B), however, makes the

specific prediction that serially successive actions that are bound under a shared motor plan

170   should exhibit a correlation in their responses over time, as a consequence of arising from a

171   common, high-level motor plan (Figure 1C). For an index of binding, we used the

172   autocorrelation of RTs during the last trial block for both groups (Verstynen et. al. 2012). Figure

173   3 shows the autocorrelation functions for early (Day 1), middle (Day 12), and late (Day 24)

174   stages of practice for the Trained (Figure 3A) and Control (Figure 3B) groups separately.

175   Participants in the Trained group showed no evidence of an autocorrelation in their RTs at Day

176   1; however, by the middle of training a pronounced autocorrelation of temporally adjacent

177   responses emerged that remained steady by the last day of practice. As expected, the Control

178   group did not show any autocorrelation structure in RTs at any point during training, indicative

179   of a lack of binding across responses.

180   We next examined the RT correlations of responses to each item in the 32-item sequence

181   on each cycle of the sequence production. Before practice, this 32x32 correlation matrix does not

182   show much structure, with all items approximately equally uncorrelated (Figure 3C). After

183   training, a clear structure in the correlations emerged, with local clusters of correlated responses

184   found along the diagonal of the matrix (Figure 3D). If these clusters of correlated responses in

185   the sequence reflect the inter-finger transition probabilities (Figure 3E), then the pairing

186   frequency of individual fingers should determine the degree of similarity between finger

187   responses. The similarity between the observed correlations and expected correlations based on

188   the pairwise frequencies (Figure 3F) was computed using the mean squared error (MSE). The

189   mean observed correlation matrix across all subjects on the final day of training is shown in

190   Figure 3G. There was increased similarity between the observed and expected correlations across

191   days (Figure 3H) in the Trained group, but the structure in the Control group remained

192   unchanged, resulting in a significant group by time interaction, $F(368,23) = 1.90$, $p = 0.0079$.

9
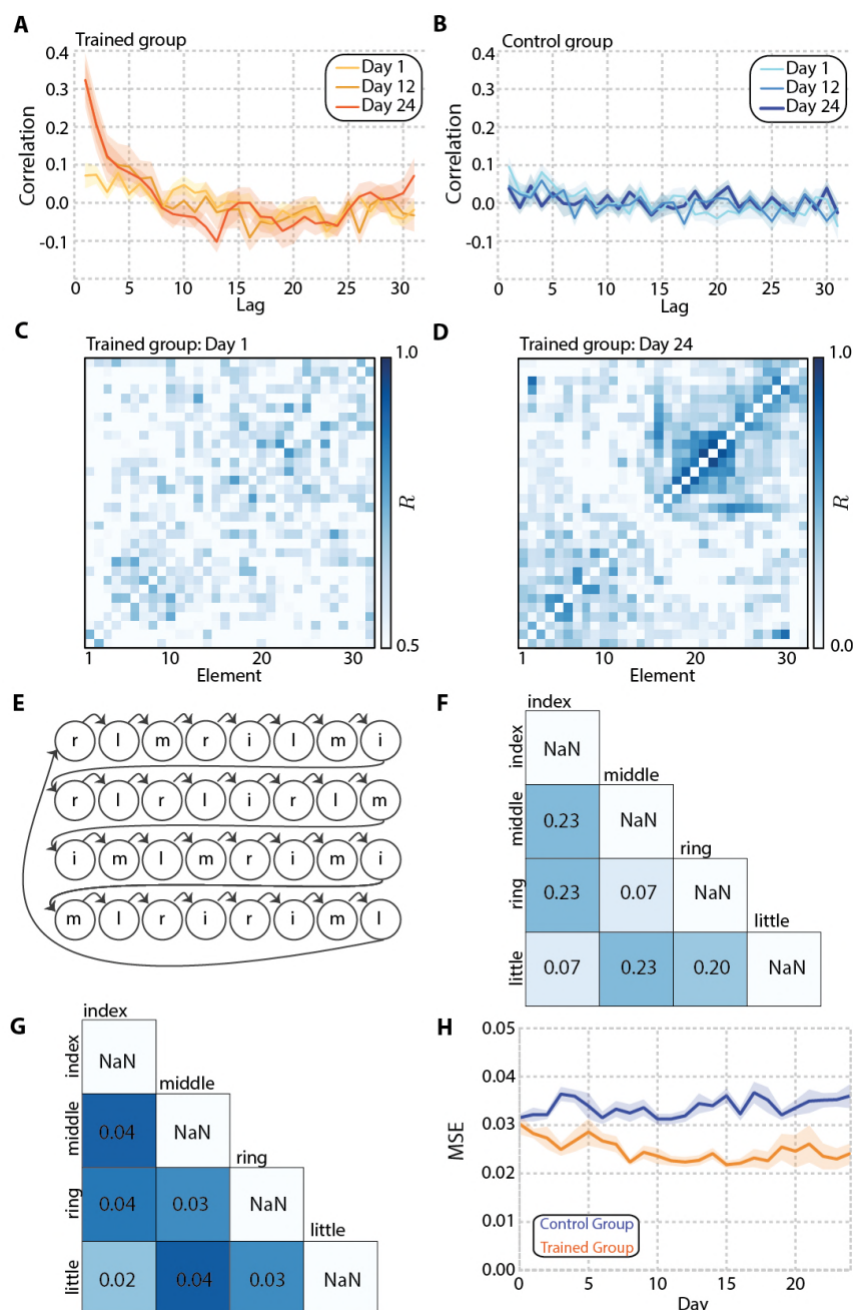
193
194 **Figure 3:** *Binding in behavioral responses.* **A,B** *Mean autocorrelation function for lags 1-31*
195 *during early (day 1), middle (day 12) and late training (day 24) for the Control group (A) and*
196 *Trained group (B). Shaded regions show standard error of the mean.* **C,D**. *Average correlation*
197 *between each element in the sequence during the final trial block for the Trained group, during*
198 *Day 1 (C) and Day 24 (D).* **E**. *The 32 element sequence showing frequency of each finger*
199 *transition (i-index, m-middle, r-ring, l-little)* **F**. *Pairwise frequencies between each finger* **G**.
200 *Average observed correlations between fingers at the end of training collapsed across subjects.*
201 **H**. *The MSE between the pairwise frequencies (panel F) and observed correlation matrix*
202 *computed separately for each subject. Smaller numbers indicate increased similarity to the*
203 *expected pairwise frequencies (panel F). Shaded regions show standard error.*

204   *Stable motor representations after training.*

205   In order to directly measure multivariate cortical representations of the individual cued

206   movements, we used a rapid-event-related fMRI design consisting of presentations of each cued

207   finger press followed by a period of fixation (Figure 4A). A regions of interest (ROI) analysis

208   was performed on the cortical motor network including primary motor cortex, M1; primary

209   somatosensory cortex, S1; dorsal premotor cortex, PMd; ventral premotor cortex, PMv;

210   supplementary motor area, SMA; and the superior parietal lobule, SPL. These regions were

211   anatomically localized using Brodmann areas extracted from Freesurfer (see Methods). These

212   regions are shown on the group average surface (Figure 4C). In each of the cortical motor ROIs,

213   we quantified the activity pattern related to each cued finger movement and then calculated a

214   cross-validated Mahalanobis distance (crossnobis) between the activity patterns for each cued

215   finger pair. If two cued fingers generate the same cortical activity patterns, then the

216   corresponding distance between them will be 0. However, if two finger movements consistently

217   generate dissimilar finger patterns, then the corresponding distance will be positive (Figure 4B).

218   Cross-validation allows us to test the value of the distance estimates directly against zero (see

219   Diedrichsen and Kriegeskorte 2017, Walther et. al. 2016, Diedrichsen et. al. 2016). The distances

220   between every possible pair of fingers is summarized in a representational dissimilarity matrix

221   (RDM) for each ROI (Figure 4D).

222   The representational structure we observed in primary motor and primary somatosensory

223   cortex qualitatively matches previous reports (Ejaz et. al. 2015), such that the index finger is

224   furthest from the little finger, while the middle and ring fingers are close together. This pattern of

225   representational distances is also similar to what is observed the other cortical motor regions,

226   although the overall between effector distances are smaller in these premotor regions (Figure

11

227   4D). To confirm that each region has reliably different representations for the fingers, we

228   computed the average cross-validated pairwise distance between all finger movements (Figure

229   4B see Methods). Average H scores greater than 0 indicate above-chance encoding (Diedrichsen

230   and Kriegeskorte 2017). Figure 4E shows the mean H distribution computed from the surface-

231   based searchlight (see Methods) across all voxels as kernel density estimates averaged across

232   subjects (one distribution per subject for each ROI). In a control region, primary auditory cortex

233   (A1), distances are symmetrically distributed about zero, indicating that one would not be able to

234   reliably decode the cued-finger movement from this region. In sensorimotor regions, the

235   distances were positively skewed indicative of cued-finger movement encoding. In order to

236   estimate the reliability of this encoding across subjects, we extracted the median distance value

237   from each distribution for each subject and ROI. A one-sample t-test on those median values

238   (one median per subject), after adjusting for multiple comparisons using a Bonferonni correction,

239   found significant separation of cued finger representations (i.e., positive average distances) in the

240   cortical sensorimotor areas, but not the A1 control region (Table 1). Thus, consistent with

241   previous studies (Ejaz et. al. 2015), the patterns of activity in the motor network can reliably

242   discriminate individual effectors.

243
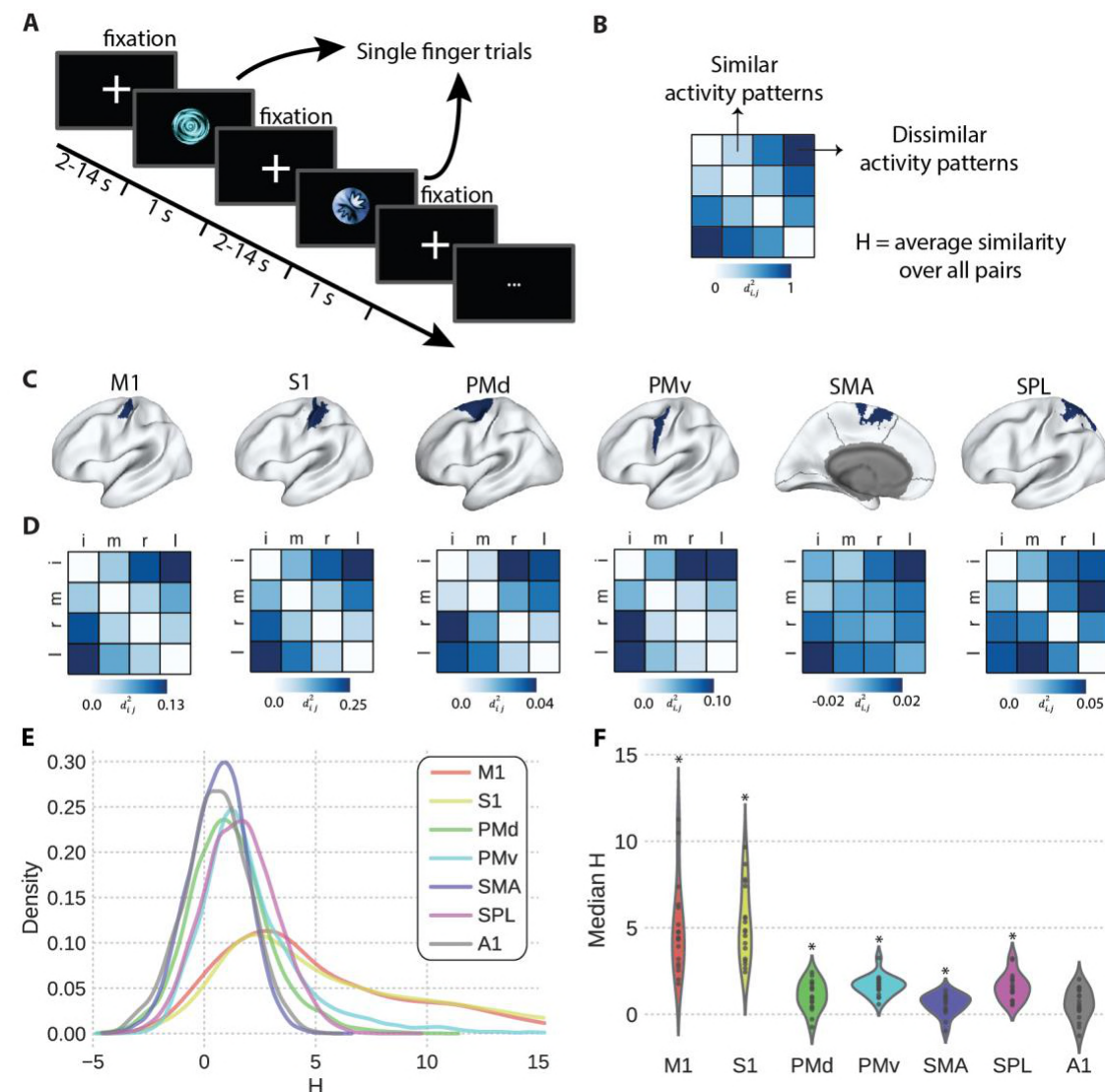
244
245 **Figure 4:** *Multivariate activity patterns during cued finger movements. **A**. fMRI task schematic.*
246 *Participants executed single finger movements on the button glove following a variable period of*
247 *fixation. The cue-finger mapping was identical to that used during the training. **B**. Example of a*
248 *representational dissimilarity matrix showing similar finger patterns that result in small*
249 *distances and dissimilar finger patterns that result in large distances. The average crossnobis*
250 *similarity (H) was used as a test statistic for assessing decoding in each ROI and for assessing*
251 *representational plasticity. **C**. Regions of interest masks overlaid in blue on the group average*
252 *surface. **D**. Average representational dissimilarity matrices for each region. Each colored*
253 *square within the RDM indicates the distance between those two fingers (i=index, m=middle,*
254 *r=ring, l=little) **E**. Average kernel density estimates of H across all subjects and all voxels in*
255 *primary motor cortex (M1), primary somatosensory cortex (S1), premotor dorsal cortex (PMd),*
256 *premotor ventral cortex (PMv), superior parietal lobule (SPL), supplementary motor area*
257 *(SMA), and primary auditory cortex (A1). **F**. Violin plots show the distributions of median H*
258 *values across subjects. Black circles inside plots show individual data. Asterisks indicate*
259 *significance at α = 0.05 after correcting for multiple comparisons (Bonferonni).*

13

| Region	Mean	t(17)	p-value	95% CI
M1	4.92	7.91	*4.23×10^{-7}	3.61, 6.23
S1	5.23	10.13	*1.28×10^{-8}	4.14, 6.32
PMd	1.07	5.30	*5.83×10^{-5}	0.64, 1.49
PMv	1.66	12.06	*9.21×10^{-10}	1.37, 1.95
SMA	0.57	4.08	*7.75×10^{-4}	0.28, 0.87
SPL	1.57	8.44	*1.74×10^{-4}	1.18, 1.97
A1	0.57	2.78	0.013	0.14, 1.01

260 *Table 1: Column "mean" indicates the average median H value in each region. T-*
261 *statistics computed from one-sided t-test.* indicates significance after correcting for*
262 *multiple comparisons.*

263
264   To determine whether the emergence of binding in the behavioral responses coincides

265 with alterations of these representational distances of individual cued actions, we measured how

266 average distances changed for each cortical motor ROI before and after training. More

267 specifically, if binding results in the representations of frequently paired actions becoming more

268 similar (Figure 1D), then distances between frequently paired movements would decrease after

269 practice only in the Trained group. When looking at all pairwise distances (Figure 5A) we were

270 unable to find a reliable influence of sequence training on the average pattern distances in any

271 cortical motor region (Figure 5B). In most areas, the distances decreased only marginally for

272 both Trained and Control groups together, but the finger patterns remained largely separable,

273 with patterns exhibiting a high degree of stability. Across all regions, we failed to detect a

274 reliable interaction between group and time that would be indicative of a training effect in

275 representational distances (all p>0.26, full statistics reported in Table 2). In order to evaluate the

276 evidence in support of the null hypothesis that the interaction is not present, we conducted a JZS

277 Bayes Factor (BF) ANOVA with uniform prior across all models (JASP Team, 2017, jasp-

278 stats.org) and found evidence in support of the null model that training does not influence

279   distances. The BF's ranged from 0.33-0.36 (Table 2), which can be considered positive evidence

280   in support of the Null hypothesis (Kaas & Raftery, 1995).
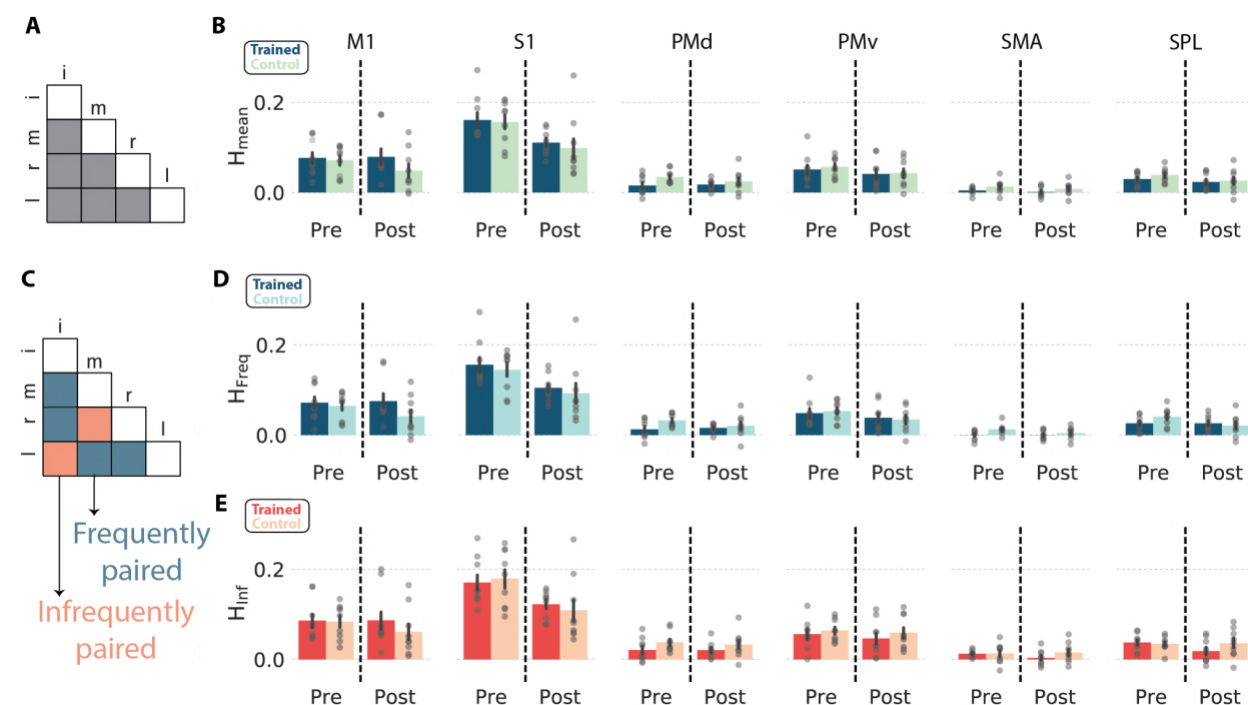
281
282   **Figure 5:** *Stable representational distances after training.* **A.** *Pairwise finger distances included*
283   *in overall distance analysis.* **B**. *Bar plots show mean ROI H values in the pre- and post-training*
284   *scans separately for each group. Error bars show standard error. Gray circles are individual*
285   *data points.* **C**. *Finger pair frequencies were asymmetrically distributed in the trained sequence*
286   *(see Figure 3F). Some finger pairs, e.g. index and little were infrequently paired, whereas other*
287   *finger pairs e.g. index and middle were frequently paired.* **D,E**. *Bar plots show mean H for*
288   *frequent pairs B (panel D) and infrequent pairs (panel E) in the Pre and Post scans separately*
289   *for each group. Error bars show standard error. Gray circles are individual data points. No*
290   *comparison was found to be statistically significant at α=0.05.*
291
292
293
294
295
296
297
298
299
300
301
302

Region	F(1,16)	p-value	Inclusion BF
M1	1.35	0.26	0.348
S1	0.086	0.77	0.349
PMd	0.74	0.40	0.349
PMv	0.066	0.80	0.367
SMA	.042	0.84	0.333
SPL	0.34	0.57	0.35

303 ***Table 2:*** *F-statistics and p-values for testing significance of interaction effect (group x time)*
304 *from repeated measures ANOVA for mean distances. Inclusion Bayes Factor (BF) is the ratio of*
305 *the posterior over the prior probability of the model including the interaction term. BF<1*
306 *provide evidence that interaction effect is not present.*

307
308   Of course, looking at changes in overall representational distances my not be sensitive

309   enough to pick up changes in the representational distances of only a few finger pairs. The

310   simple plasticity model we proposed in the Introduction predicts that the greatest plasticity

311   should be observed in the finger pairs most often executed together in the sequence. If the

312   distances decreased for the more frequently paired effectors, but increased for the less frequently

313   paired effectors this may result in a net change for the overall average distance near 0. To

314   explore this possibility, we re-analyzed the distance changes by looking at the frequently and

315   infrequently occurring finger pairs in the sequence structure itself (Figure 3F). Based on the

316   pairing frequencies, we identified four frequent finger pairs and two infrequent pairs (Figure 5C).

317   However, much like the overall distance patterns, we were unable to resolve focal changes in

318   representational distances in either of the most frequently (Figure 5D) or infrequently (Figure

319   5E) paired effectors. Across all regions, two way repeated measures ANOVA indicated no

320   significant group-by-time interaction for either frequently paired (all $p > 0.26$, full statistics

321   provided in Table 3) or infrequently paired fingers (all $p > 0.13$, full statistics provided in Table

322   4). The Bayesian ANOVA revealed anecdotal evidence in favor of the null hypothesis for both

323   the frequently (BFs: 0.68-0.89, Table 3) and infrequently (BFs: 0.53-0.60, Table 4) paired

324   fingers.

Region	F(1,16)	p-value	Inclusion BF
M1	1.36	0.26	0.87
S1	0.00065	0.98	0.86
PMd	1.27	0.28	0.89
PMv	0.27	0.61	0.68
SMA	1.05	0.32	0.83
SPL	2.86	0.11	0.84

325   ***Table 3****: F statistics and p-values for testing significance of interaction effect (group x time)*
326   *from repeated measures ANOVA for frequently paired fingers. Inclusion Bayes Factor (BF) is*
327   *the ratio of the posterior over the prior probability of the model including the interaction term.*
328   *BF<1 provide evidence that interaction effect is not present.*

Region	F(1,16)	p-value	Inclusion BF
M1	1.16	0.30	0.54
S1	0.69	0.42	0.60
PMd	0.070	0.80	0.54
PMv	0.083	0.78	0.53
SMA	1.05	0.32	0.56
SPL	2.53	0.13	0.54

329   ***Table 4:*** *F statistics and p-values for testing significance of interaction effect (group x time)*
330   *from repeated measures ANOVA for the infrequently paired fingers. Inclusion Bayes Factor (BF)*
331   *is the ratio of the posterior over the prior probability of the model including the interaction term.*
332   *BF<1 provide evidence that interaction effect is not present.*

333

334   **DISCUSSION**

335   Here we examined whether the binding of serial actions during long-term sequence learning

336   alters the cortical representations of individual cue-response pairings. We found that during

337   sequence production, temporally adjacent responses develop a high degree of correlation in their

338   response speeds, consistent with participants binding multiple responses together under a unified

339   command so as to reduce computational complexity (see also: Verstynen et. al. 2012, Ramkumar

17

340 et. al. 2016, Lynch et. al. 2017). Using a multivariate pattern analysis approach, based on the

341 cross-validated Mahalanobis estimator, we also replicated previous studies showing that cortical

342 motor areas reliably distinguish between activation patterns of individually cued finger responses

343 (Ejaz et. al. 2015). We were, however, unable to find evidence for learning-related changes in

344 this representational structure of cued finger responses in any of the cortical regions tested.

345 Taken together, these findings show that the process of binding actions into chunked sets during

346 long-term skill learning does not impact the representation of individual cued actions, suggesting

347 that binding relies on changing more complex levels of representation beyond individual

348 movements.

349   At first glance, the absence of plasticity in population level representations of individual

350 actions that we observed appears to be incompatible with previous reports of plasticity in

351 sensorimotor cortex. Kolansinki and colleagues (2016) found that the representational distances

352 of individual fingers shifted in S1 after physically yoking two fingers together for a period of 24

353 hours. In their study, the sensory representations of the two yoked fingers remained spatially and

354 temporally identical, however the unyoked fingers altered their distances, suggesting a possible

355 compensatory effect in the sensory representations themselves. In contrast, our task relied on

356 training associations between temporally independent movements in a specific context. It is

357 possible that, had we trained on chord-like movements, where multiple fingers are

358 simultaneously engaged (Verstynen et. al. 2005), for a longer period of time, we might have

359 observed similar changes in cortical sensorimotor representations, a hypothesis that is left open

360 to future studies.

361   Alternatively, there is a strong rationale for why single effector representations would

362 remain stable in cortical sensorimotor networks, particularly motor execution areas like M1, after

363   long-term sequence learning. First, binding responses at the execution level may be a

364   maladaptive strategy for maintaining a flexible movement repertoire (Lashley, 1951). For

365   example, if index finger movements were consistently bound with middle finger movements

366   because a single daily task required them to work together in sequential fashion, then they might

367   exhibit a prepotent response in inappropriate contexts. In order to maximize flexibility, it would

368   be beneficial for the movements to be bound at a more abstract motor planning stage, upstream

369   from execution processes. Second, practice may involve refining the control of execution-level

370   representations without necessarily impacting the representations themselves. This would

371   suggest that the process of binding during the consolidation of complex movement sequences is

372   dependent on plasticity mechanisms at hierarchically higher level of processing (Wong et. al.

373   2015).

374   Of course, it is possible that there is plasticity in the representations of individual

375   sensorimotor effectors during long-term sequence learning, but limitations in our experimental

376   design may preclude identifying those changes. First, while the duration of training we used was

377   longer than many sequence learning experiments in humans, five weeks may still not be enough

378   time to lead to measurable representational changes in primary motor cortex. This concern is

379   tempered by the fact that we were able to show strong evidence of action binding in the

380   behavioral responses. Second, we could not look at finger representations in the striatum, where

381   there is some evidence for binding (Jin et. al. 2014, Wymbs et. al. 2012) as the voxel sizes in this

382   study were too large to examine those representational structures. Future studies at a higher MRI

383   field strength (e.g., 7T) may afford a better spatial resolution for picking up plasticity of

384   sensorimotor representation in the striatum.

385   Despite these limitations, our experiment clearly shows that five weeks of training on a

386   complex unimanual sequence task does not alter the sensorimotor representations of individual

387   effectors despite clear evidence of binding in the motoric actions. This suggests that execution

388   level representations remain stable during learning and that proficiency is likely controlled by a

389   higher level within the motor hierarchy.

390

391   **MATERIALS AND METHODS**

392   *Participants*

393   Eighteen right-handed participants (6 female, mean age: 26 years) were recruited locally from

394   Carnegie Mellon University (CMU) and the University of Pittsburgh. Two authors (PB and TV)

395   were included in the sample. All participants provided informed consent and were financially

396   compensated for their time. All experimental protocols were approved by the Institutional review

397   board at CMU.

398

399   *Serial reaction time task*

400   Participants were trained for 25 nonconsecutive days on a variant of the serial reaction time task

401   (Nissen and Bullemer, 1987). All experimental procedures were performed on a laptop running

402   Ubuntu 14.04. At the beginning of each training session, participants were instructed to place

403   their right hand over the "h" (index),"j" (middle), "k" (ring), and "l" (pinky) key. Each trial

404   consisted of a presentation of one of four unique fractal cues appearing on a black background.

405   Each cue was uniquely mapped to one of four keys on the keyboard (Figure 2A). The trial ended

406   either when the participant executed a response or once the maximum response window expired

407   (see below), depending on which event happened first. After a trial termination, the next cue was

408   presented after a 250 ms inter-trial interval. Each trial block consisted of 256 trials and was

409   followed by a rest period where the mean response time (RT) and accuracy for that block was

410   provided to the participant. On each training day, participants completed 1792 trials, separated

411   into 7 trial blocks. RT was calculated as the delay between stimulus presentation and a key press.

412   Stimulus presentation and recording was controlled with custom written software in Python

413   using the open source Psychopy package (Peirce, 2007). The software used for training is

414   available on GitHub (CoAxLab, n.d.).

415   Prior to the first session, subjects were assigned to either a Trained group (n=9) or a

416   Control group (n=9). For participants in the Trained group, trial blocks were separated into two

417   types: blocks of pseudo randomly ordered cues (Random; blocks 1,2,6) or blocks of

418   deterministically ordered cues following an embedded 32-element sequence (Sequence; blocks

419   3,4,5,7). Figure 2B shows the blockwise structure for a single subject in the Trained group. Trials

420   during the Random blocks were constrained such that repeated presentations of the same cue

421   were excluded. This was done so that Random trial blocks would appear more similar to the

422   Sequence trial blocks. The 32 element sequence presented on Sequence blocks consisted of the

423   following key presses: 3-4-2-3-1-4-2-1-3-4-3-4-1-3-4-2-1-2-4-2-3-1-2-1-2-4-3-1-3-1-2-4 using

424   the mapping (1-index finger, 2-middle finger, 3-ring finger, 4-little finger). Each Sequence block

425   began in a random position of the sequence. For the first 2 blocks, the response threshold for

426   each trial was set to 1000 ms. To encourage faster responses, the response window of blocks 3-5

427   was adaptively controlled such that the response window on one trial block was the mean plus

428   one standard deviation of the RTs from the previous trial block. If that value fell below 200 ms

429   or if the accuracy on the preceding block was less than 75%, the threshold was reset to 1000 ms.

430   The threshold was removed for the final probe blocks (6 and 7) so that participants could move

431   as quickly as they chose. For the Control group, the procedure was nearly identical to the Trained

432   group, with the exception that all 7 blocks consisted of pseudorandomly ordered trials, i.e. there

433   was no exposure to Sequence blocks.

434

435   *Analysis of training data*

436   Python code and source data to generate all figures is publicly available on GitHub

437   (https://github.com/CoAxLab/binding_manuscript). All behavioral analysis during training

438   focused on responses during the last two trial blocks (probe blocks) when no adaptive response

439   window was applied: Random and Sequence conditions for the Trained group, Random and

440   Random conditions for the Control group. Differences in response time (RT) and accuracy

441   (percent correct responses) were measured as the difference in the means between the last two

442   blocks, normalized by the standard deviation of values in trial block 6, i.e., z-scored difference in

443   performance (Verstynen et al., 2012). In the Trained group this reflects the sequence specific

444   change in performance on each day. Since 3 subjects completed 24/25 days of training, average

445   group visualizations are presented for day 24 so as to evaluate the same state of learning for all

446   subjects.

447   Binding was measured by computing the autocorrelation of the series of RTs within each

448   probe trial block. The first 32 trials were excluded to remove the exponential decay as it distorts

449   the autocorrelation analysis (Verstynen et al., 2012). The linear trend was then removed by

450   regression and the residuals were used to calculate the autocorrelation function for lags 1 through

451   31, following the same procedure as described in (Verstynen et al., 2012; Lynch et al., 2017).

452   Since the autocorrelation function measures general associations across all sequential

453   lags, it is not sensitive to specific associations between individual elements, and therefore cannot

454 be used to measure binding between specific finger pairs. Therefore, we conducted a secondary

455 analysis on the same data but examined pairwise correlations between each distinct element (1-

456 32) in the sequence. Average correlations, ordered by sequence element, are shown in Figure 3C-

457 D. Binding between successive elements is reflected by increases in correlations distances before

458 compared to after training.

459   To measure how much the correlation between finger responses matches the statistical

460 structure of the trained sequence, we collapsed the elementwise correlation matrices by finger

461 identity (index, middle, ring, pinky), forming 4x4 observed correlation matrices. To measure the

462 similarity of the observed binding structure to the expected binding structure, we computed the

463 mean squared error between the finger pairing frequencies of the sequence and observed

464 correlations. This gives a normalized similarity measure for how well the pattern of correlations

465 in the behavioral responses matches the pairwise similarities of the trained sequence.

466

467 *Imaging acquisition*

468 Before and after training, all participants were scanned at the Scientific and Brain Research

469 Center at Carnegie Mellon University on a Siemens Verio 3T magnet fitted with a 32-channel

470 head coil. High-resolution T1-weighted anatomical images were collected for visualization and

471 surface reconstruction (MPRAGE, 1 mm isotropic, 176 slices). A fieldmap with dual echo-time

472 images (TR: 746 ms, TE1: 5.00 ms, TE2: 7.46 ms, 66 slices, 2 mm isotropic) was acquired to

473 correct for fieldmap inhomogeneities. For the functional imaging sessions, we acquired 241 T2*

474 weighted echo-planar imaging volumes (2 mm isotropic, TR: 2000ms, TE: 30.3 ms, MB factor:

475 3, 66 slices, A >> P, FoV: 192 mm, interleaved ascending order, flip angle: 79 deg, matrix size:

476 96x96x66, slice thickness: 2.00 mm). For the finger mapping task, we collected a total of 6 runs

477   resulting in 1446 volumes. Functional images were oriented so as to maximize coverage of the

478   entire cortex and cerebellum.

479   *Neuroimaging tasks*

480   We collected a set of finger mapping runs to estimate the activation patterns evoked by

481   performing each distinct cue-response pair in isolation (i.e. not embedded within a sequence).

482   The same stimuli from the behavioral experiments were projected on an MR-compatible LCD

483   screen mounted at the rear of the scanner. Participants could see this screen through a mirror

484   mounted on the head coil. Responses were recorded on a five-key MR compatible response

485   glove (PST Inc.) placed under the right hand. Each effector (e.g., individual cue-response

486   pairing) was presented in isolation on each trial with no structured order between trials. Thus, the

487   paradigm only measured responses to individual cued movements, not the sequence itself. Each

488   trial type was repeated 12 times per run totaling 72 trials per session. Subjects were instructed to

489   press the cued key several times following stimulus presentation until the cue disappeared from

490   the screen (1 second). Between runs, subjects were given the option to take several minutes of

491   rest.

492

493   *Imaging Analysis*

494   Functional imaging data were analyzed using SPM8 (http://www.fil.ion.ucl.ac.uk/spm/) and

495   custom Matlab and Python functions. Raw functional EPI images were realigned to the first

496   volume. No slice time correction was applied. These realigned images were then corrected for

497   field distortions using the field maps. All analyses were performed in native functional space.

498   Structural T1 images were used to reconstruct the pial and white surfaces using Freesurfer

499   (Fischl, 2012). All custom code is publicly available (CoAxLab, n.d.).

24

500   All analyses of task-related responses were performed using a region of interest (ROI)

501   approach. Anatomical ROIs were defined separately for each subject, using the surface based

502   Brodmann areas extracted from Freesurfer (Fischl et al., 2008) following similar conventions as

503   described in (Wiestler and Diedrichsen, 2013). The hand voxels of the primary motor cortex

504   (M1) were defined as the surface nodes with the highest probability of belonging to Brodmann

505   area (BA) 4, 1 cm above and below the hand knob (Yousry et al., 1997). S1 was defined as the

506   nodes in BA1 BA2, BA3a, or BA3b, 1 cm above and below the hand knob. Premotor cortex was

507   defined as the nodes belonging to BA6 medial (PMv) or lateral (PMd) to the medial frontal

508   gyrus. Supplementary motor area (SMA) was defined as the voxels in BA6 along the medial

509   wall. The Freesurfer atlas was used to define the superior parietal gyrus, as it is not defined by a

510   unique Brodmann area. As a control ROI, we extracted the voxels belonging to primary auditory

511   cortex as this region would not be expected to exhibit any significant decoding of the visually-

512   cued finger patterns. Each surface based ROI was projected back into native functional space.

513   Analysis for effector representations was performed using representational similarity

514   analysis (RSA) using the crossnobis estimator (Kriegeskorte et al., 2008; Nili et al., 2014;

515   Walther et al., 2015). A GLM with regressors for each effector was fit for each mapping run,

516   along with the six head motion regressors (x, y, z, pitch, yaw, roll). Omissions and incorrect key

517   presses were regressed out of the model. Raw time series were orthogonalized by eigenvector

518   decomposition and projected into the principal component space to minimize model bias in the

519   decoding. To estimate the differences between finger patterns, we used a cross-validated

520   Mahalanobis distance between prewhitened regression coefficients for each effector (Atsushi et.

521   al., 2017, Walther et al., 2015). The cross-validated Mahalanobis distance has the advantage over

522   other distance measures in that it is unbiased, since noise is orthogonalized across runs, resulting

25

523   in an expected distance of 0 if a voxel or region does not reliably distinguish two finger patterns

524   (Ejaz et al., 2015). The estimated distance ($\hat{d}$) between the patterns (u) of two fingers (i,j) was

525   averaged across every pair (m,l) of runs (M) resulting in (6 choose 2) = 15 folds using the

526   following equation:

527

$$\hat{d}_{i,j}^2 = \sum_{l,m;l\neq m}^{M} \frac{(u_i^m - u_j^m)^T(u_i^l - u_j^l)}{M(M-1)}$$

528   *Equation 1*

529   The pairwise distances between each of the fingers are summarized in a representational

530   dissimilarity matrix (Figure 4B). To test for encoding and plasticity within each voxel or ROI,

531   we extracted the average distance between each pair of fingers pattern (K=4) using the following

532   equation:

533

$$H = \sum_{i\neq j}^{K} \frac{d_{i,j}^2}{K^2 - K}$$

534   *Equation 2*

535   To examine the extent of finger representations across all of cortex, we conducted a surface-

536   based searchlight (Oosterhof et al., 2011), assigning every surface node an H value based on the

537   local (p=160) patterns surrounding an approximately 10 mm radius. Values for the number of

538   voxels (p) and radius were chosen based on previous studies (Yokoi et. al. 2017). This

539   searchlight approach enabled us to examine the entire H distribution across all voxels in each of

540   the ROIs to confirm that each region reliably discriminated individual effectors. Due to the

541   observed positive skew, we extracted the median H for all regions across all subjects and

542   conducted a one sample t-test against 0, in order to establish whether a region reliably decoded

543   the single finger movement representations. For tests of plasticity, changes in representational

544   distances were compared using the patterns across the top 150 voxels from each ROI, rank-

545   ordered by average distance, similar to the number of voxels used in previous studies (Wiestler

546   and Diedrichsen, 2013), because representational geometries are highly sensitive to the number

547   of voxels that make up a pattern (Oosterhof et al., 2011). We computed H separately for the pre

548   and post training sessions and each ROI. A repeated measures ANOVA was used to examine the

549   influence of training on distances in each ROI. Bayesian repeated measures ANOVA with a JZS

550   prior over all models was used to determine the inclusion Bayes Factor to measure the extent to

551   which the data supported inclusion of the interaction effect (JASP Team, 2017, jasp-stats.org).

552   The guidelines in (Kass and Raftery, 1998) were used to interpret the weight of the evidence in

553   support of the null hypothesis.

554

References

Acuna D.E., Wymbs N.F., Reynolds C.A., Picard N, Turner R.S., Strick P.L., Grafton S.T., Kording K (2014) Multi-faceted aspects of chunking enable robust algorithms. *Journal of neurophysiology*, 112(8), 1849–1856.

Beukema P, Verstynen T. (2018). Predicting and Binding: interacting algorithms supporting the consolidation of sequential motor skills. *Current Opinion in Behavioral Sciences* 20:98-103

CoAxLab (n.d.) CoAxLab/binding_manuscript: source data and code for stable representations manuscript. Available at: https://github.com/CoAxLab/binding_manuscript

Diedrichsen, J., & Kriegeskorte, N. (2017). Representational models: A common framework for understanding encoding, pattern-component, and representational-similarity analysis. *PLoS computational biology*, *13*(4), e1005508.

Diedrichsen, J., & Kornysheva, K. (2015). Motor skill learning between selection and execution. *Trends in cognitive sciences*, *19*(4), 227-233.

Diedrichsen J, Zareamoghaddam H, Provost S. The distribution of crossvalidated mahalanobis distances. ArXiv. 2016

Ejaz N., Hamada M., & Diedrichsen J. (2015) Hand use predicts the structure of representations in sensorimotor cortex. *Nature Neuroscience* 18(7), 1034-1040.

Fischl B. (2012). FreeSurfer. *Neuroimage* 62:774–781.

Fischl B., Rajendran N., Busa E., Augustinack J., Hinds O., Yeo B.T., Mohlberg H., Amunts K., & Zilles K (2008) Cortical folding patterns and predicting cytoarchitecture. *Cerebral Cortex* 18(8), 1973–1980.

JASP Team (2017). JASP (Version 0.8.4). Retrieved from https://jasp-stats.org/

Jin, X., Tecuapetla, F., & Costa, R. M. (2014). Basal ganglia subcircuits distinctively encode the parsing and concatenation of action sequences. *Nature neuroscience*, *17*(3), 423-430.

Kass, R. E., & Raftery, A. E. (1995). Bayes factors. *Journal of the american statistical association*, *90*(430), 773-795.

Kolasinski J., Makin T.R., Logan J.P., Jbabdi S., Clare S., Stagg C.J., & Johansen-Berg H. (2016). Perceptually relevant remapping of human somatotopy in 24 hours. *eLife* (5).

Kriegeskorte N., Mur M., Bandettini P. (2008). Representational similarity analysis - connecting the branches of systems neuroscience. *Frontiers in systems neuroscience* 2.

Lashley, K.S. (1951). The problem of serial order in behavior. In: *Cerebral mechanisms in behavior*, pp 112–136.

Lynch B., Beukema P., Verstynen T. (2017). Differentiating Visual from Response Sequencing During Long-term Skill Learning. *Journal of cognitive neuroscience* 29(1), 125–136.

Nili H., Wingfield C., Walther A., Su L., Marslen-Wilson W., Kriegeskorte N. (2014). A toolbox for representational similarity analysis. *PLoS computational biology* 10(4):e1003553.

Nissen M.J., Bullemer P. (1987). Attentional requirements of learning: Evidence from performance measures. *Cognitive psychology,* 19(1), 1–32.

Nudo R.J., Milliken G.W., Jenkins W.M., Merzenich M.M. (1996). Use-dependent alterations of movement representations in primary motor cortex of adult squirrel monkeys. *Journal of Neuroscience,* 16(2), 785–807.

Oosterhof N.N., Wiestler T., Downing P.E., Diedrichsen J. (2011). A comparison of volume-based and surface-based multi-voxel pattern analysis. *Neuroimage*, 56(2), 593–600.

Peirce J.W. (2007). PsychoPy-Psychophysics software in Python. *Journal of neuroscience methods,* 162(1), 8–13.

Ramkumar P., Acuna D.E., Berniker M., Grafton S.T., Turner R.S., Kording K.P. (2016) Chunking as the result of an efficiency computation trade-off. *Nature communications,* 7:12176.

Verstynen T., Diedrichsen J., Albert N., Aparicio P., Ivry R.B. (2005). Ipsilateral motor cortex activity during unimanual hand movements relates to task complexity. *Journal of neurophysiology,* 93(3), 1209–1222.

Verstynen T.D., Phillips J., Braun E., Workman B., Schunn C., Schneider W. (2012) Dynamic Sensorimotor Planning during Long-Term Sequence Learning : The Role of Variability, Response Chunking and Planning Errors. *PLoS One* 7:e47336.

Verwey W.B. (1996). Buffer loading and chunking in sequential keypressing. *Journal of Experimental Psychology: Human Perception and Performance*, 22(3):544–562.

Walther A., Nili H., Ejaz N., Alink A., Kriegeskorte N., Diedrichsen J. (2015). Reliability of dissimilarity measures for multi-voxel pattern analysis. *Neuroimage,* 137, 188-200.

Wiestler T., Diedrichsen J. (2013). Skill learning strengthens cortical representations of motor sequences. *eLife*, 2013:1–20.

Wong, A. L., Lindquist, M. A., Haith, A. M., & Krakauer, J. W. (2015). Explicit knowledge enhances motor vigor and performance: motivation versus practice in sequence tasks. *Journal of Neurophysiology, 114*(1), 219-232.

Wymbs N.F., Bassett D.S., Mucha P.J., Porter M.A., Grafton S.T. (2012). Differential recruitment of the sensorimotor putamen and frontoparietal cortex during motor chunking in humans. *Neuron*, 74(5), 936–946.

627   Yokoi A, Diedrichsen J. 2017. Does human primary motor cortex represent sequences of finger
628   movements? bioRxiv, 157438
629
630   Yousry T.A.., Schmid U.D., Alkadhi H., Schmidt D., Peraud A., Buettner A., Winkler P. (1997)
631   Localization of the motor hand area to a knob on the precentral gyrus. A new landmark.
632   *Brain: a journal of neurology*, 120(1), 141–157.